



Contents lists available at ScienceDirect

Bioorganic & Medicinal Chemistry Letters

journal homepage: www.elsevier.com/locate/bmcl

Indolinone based LRRK2 kinase inhibitors with a key hydrogen bond

Stefan Göring^{a,†}, Jean-Marc Taymans^b, Veerle Baekelandt^b, Boris Schmidt^{a,*}^a Clemens Schöpf—Institute of Organic Chemistry and Biochemistry, Technische Universität Darmstadt, 64287 Darmstadt, Hessen, Germany^b KU Leuven, Laboratory for Neurobiology and Gene Therapy, Leuven B-3000, Belgium

ARTICLE INFO

Article history:

Received 11 June 2014

Revised 20 August 2014

Accepted 21 August 2014

Available online 29 August 2014

Keywords:

Parkinson's disease

Leucine-rich repeat kinase 2 (LRRK2)

LRRK2-inhibitors

Zebrafish phenotype

ABSTRACT

The most prevalent leucine-rich repeat kinase 2 (LRRK2) mutation G2019S is associated with Parkinson's disease (PD). It enhances kinase activity and has been identified in both familial and sporadic cases. Kinase activity was reported to be required for LRRK2 mutants to exert their toxic effects. Hence LRRK2 kinase inhibition may be a promising therapeutic target for PD. Here we report on the discovery and characterization of indolinone based LRRK2 inhibitors. Indolinone **15b**, the most potent and selective inhibitor of the present series, is characterized by an IC_{50} of 15 nM against wild-type LRRK2 and 10 nM against the LRRK2 G2019S mutant, respectively. Compound **15b** was further evaluated in a kinase panel including 46 human protein kinases and in a zebrafish embryo phenotype assay, which enabled toxicity determination in whole organisms.

© 2014 Elsevier Ltd. All rights reserved.

Parkinson's disease (PD) is after Alzheimer's disease the second most common, age related, neurodegenerative disorder, affecting about 2% of the population older than 60 years.¹ It is characterized clinically by a number of symptoms, for example, tremor at rest, bradykinesia, rigidity and postural instability. Specific neuropathological hallmarks for PD are the neuronal cell loss in dopaminergic neurons of the substantia nigra pars compacta and the formation of intracellular fibrils and Lewy bodies in the surviving neurons. A major component of Lewy bodies is α -synuclein.² To date the underlying molecular mechanism of PD remains poorly understood and there is no cure for this disease.

The leucine-rich repeat kinase 2 (LRRK2) is a multi-domain protein and consists of 2527 amino acids. Several independent domains are known for the LRRK2 protein including both a serine/threonine kinase and a GTPase domain. Several mutations have been identified inside the protein, at least five of them (R1441C, R1441G, Y1699C, G2019S and I2020T) are currently assumed to be pathogenic and are localized in the catalytic core.^{3–5} The most prevalent mutation is the glycine to serine amino acid substitution, which is present in more than 85% of familial PD patients carrying LRRK2 mutations.⁶

Converging studies point to the inhibition of LRRK2 kinase activity as a therapeutic concept. First, the G2019S mutation in the kinase domain increases the kinase activity 2- to 3-fold

compared to its wild type counterpart.^{7–9} This effect may guide the pharmacological development of kinase inhibitors for a potential PD therapy. Second, the cellular toxicity of acute overexpression of LRRK2 clinical mutants is ablated when these mutations are combined with mutations inactivating the kinase activity, both in cell culture and primary neurons,^{7,10} as well as in viral vector mediated brain overexpression in rodents.^{11,12} Although pharmacological studies have begun to indicate that LRRK2 kinase inhibition may be beneficial in reversing LRRK2 mediated toxicity,¹² further confirmation studies with more potent and specific LRRK2 inhibitors are required.^{13,14}

At present different chemotypes of LRRK2 inhibitors are known (Fig. 1). Compounds of several structural families as indolinone **1** (GW5074),¹² the diaminopyridines **2** (LRRK2-IN-1),¹⁵ **3** (TAE684)¹⁶ and **4** (HG-10-102-01),¹⁷ the cinnoline derivative **5**¹⁸ or the triazolopyridine **6**¹⁹ are potent LRRK2 kinase inhibitors. Especially the LRRK2 inhibitor HG-10-102-01 **4** exhibited good selectivity and pharmacokinetic properties regarding brain penetration and dephosphorylated Ser910 and Ser935 in tissues including kidney, spleen and brain.¹⁷

Nevertheless, the ideal LRRK2 inhibitor has not yet been reported. Thus the interest to explore activities of multiple classes of compounds that provide desirable characteristics such as potency, selectivity, cellular activity and brain penetrance, to name a few, remains in focus.³

In a previous study we have reported the inhibition of the FMS-like tyrosine kinase-3 (FLT-3) by substituted indolinones.²⁰ FLT-3 is involved and aberrantly active in acute myeloid leukemia (AML).^{21,22} Working on FLT-3 inhibitors we have identified a highly

* Corresponding author. Tel.: +49 6151 163075, +49 6151 164531; fax: +49 6151 163278.

E-mail address: schmidt_boris@t-online.de (B. Schmidt).

† Tel.: +49 6151 164531; fax: +49 6151 163278.

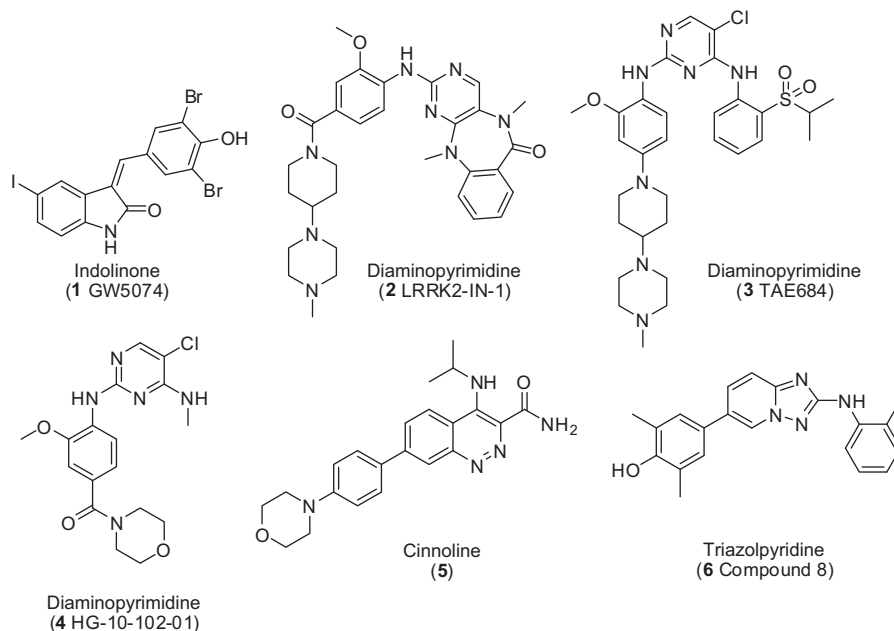


Figure 1. Selected chemotypes as lead structures for the development of new LRRK2 inhibitors.^{12,15–19}

active and selective compound based on the indolinone scaffold (Fig. 2). The indolinone **7** exhibited an IC_{50} value for FLT-3 in the low nanomolar range. Additionally, the selectivity of indolinone derivative **7** was determined at a concentration of $1 \mu\text{M}$ against 50 human protein kinases.²⁰ Beside FLT-3 only two other kinases (MAP4K4 and JAK3) were also inhibited by this compound. Unfortunately, LRRK2 was not part of this kinase screening. Due to the structural analogy of compound **7** to the known LRRK2 inhibitors **1** (GW5074) and Sunitinib, a well-known multi-kinase inhibitor, we refocused our interest on the inhibition of LRRK2. A recent publication by Novartis confirmed the efficiency of indolinones as selective and brain penetrant LRRK2 inhibitors.²³

In the absence of a full-length LRRK2 crystal structure analysis, the use and construction of LRRK2 homology models is the key for structure based design. In order to gain insight in how the indolinone derivative **7** interacts with the ATP-binding pocket of LRRK2 we performed docking studies of **7** in a LRRK2 homology model. Based on the sequence identity with the LRRK2 kinase domain, the tyrosine-kinase like kinase B-Raf (PDB 4DBN) was selected as template to model LRRK2 kinase. The alignment between the LRRK2 kinase domain and B-Raf kinase was performed using the automatic mode of the Swiss Model server.^{24,25} The final homology model was visualized using Molegro Virtual Docker 6. The validity of docking compounds onto a modeled structure of LRRK2 kinase was recently demonstrated using a kinome-wide kinase inhibitor panel correlating docking scores to compound.²⁶

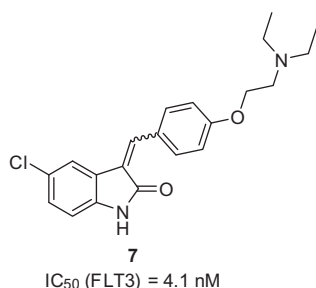


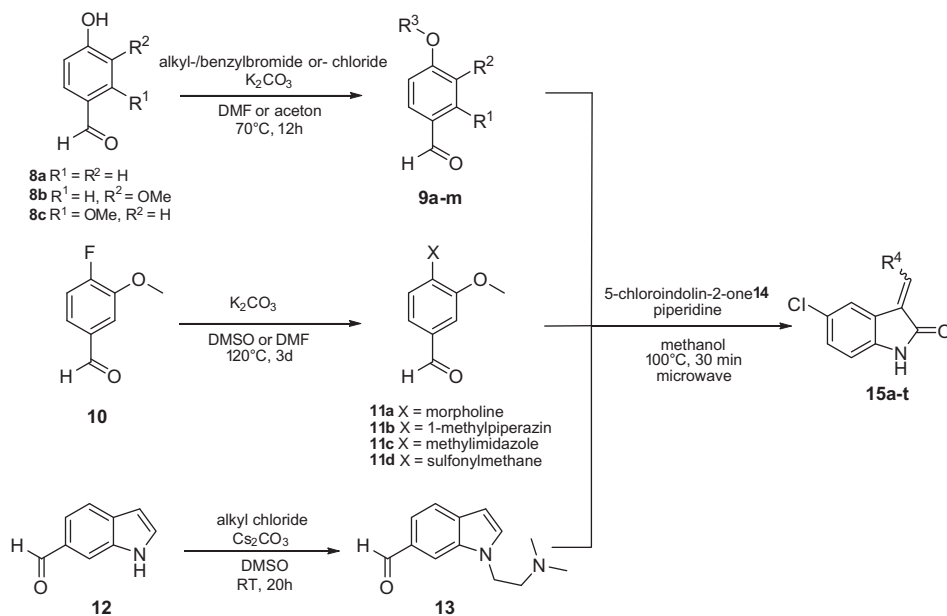
Figure 2. Highly potent and selective indolinone inhibitor for FLT3.²⁰

This model revealed that the indolinone moiety favorably interacts with the backbone of LRRK2 ATP pocket. Additionally an important interaction was observed with the diethylaminoethoxy anchor. The nitrogen of the diethylamine group interacts with the rear of the ATP-binding pocket and forms a strong hydrogen bond to K1906 in addition to several hydrophobic interactions with amino acids in the close surroundings of the phenol moiety. To confirm the docking results of indolinone derivative **7** in the LRRK2 homology model the potency of this compound was determined against LRRK2 in an in vitro peptide substrate based kinase activity assay at concentrations of 10 and $1 \mu\text{M}$ (assay information is available in the [Supplementary data](#) and referenced in [27](#) and [26](#)). Those results agreed with our hypothesis and previous docking studies. Thus, indolinone **7** reduces in vitro LRRK2 activity by more than 50% relative to control for both concentrations ([Table 1](#)). At 10 and $1 \mu\text{M}$ of compound, residual LRRK2 kinase activities of 12% and 11% were observed, respectively. To assess the activity of compound **7** more precisely we determined the IC_{50} value additionally. An IC_{50} value of $0.265 \mu\text{M}$ clearly demonstrated the submicromolar potency of compound **7** and consequently indolinones as LRRK2 inhibitors. Based on these encouraging results indolinone **7** was an attractive lead structure for further structure–activity–relationship (SAR) optimization.

Additional indolinone derivatives were synthesized by known conditions using a Knoevenagel condensation between indolinone and the corresponding aldehydes in methanol and a catalytic amount of piperidine. The Knoevenagel condensation is a reliable and quick method to establish chemical diversity for the variation of the SAR study based on compound **7**. The synthesis is outlined in [Scheme 1](#). The first step provides the aldehydes for the subsequent Knoevenagel condensation. Hence, the alkyl and aryl benzyl halides were connected with derivatives of 4-hydroxybenzaldehydes **8a–c**

Table 1
LRRK2 activity of compound **7**

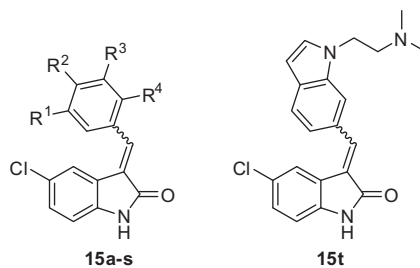
Compound	LRRK2 activity		IC_{50}
	10 μM of compd	1 μM of compd	
7	12%	11%	$0.265 \mu\text{M}$



Scheme 1. Synthesis of aldehydes derivatives for the following Knoevenagel condensation.

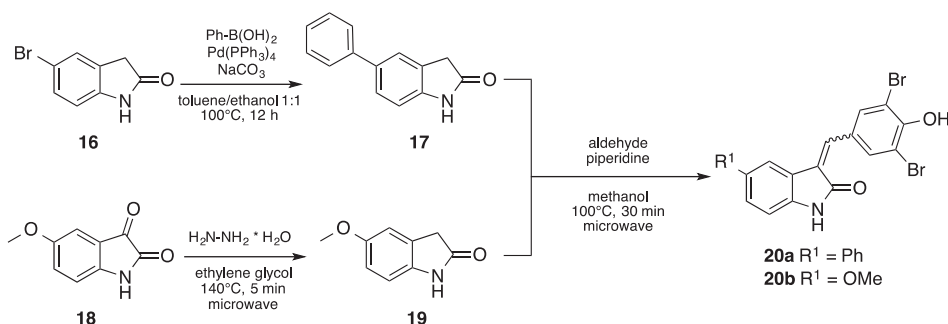
Table 2

Synthesized indolinone derivatives and their in vitro LRRK2 inhibitory activity



Compound	R ¹	R ²	R ³	R ⁴	LRRK2 activity		IC ₅₀ (μM)
					10 μM of compd (%)	1 μM of compd (%)	
Staurosporine*	—	—	—	—	2	5	—
LRRK2-IN-1*	—	—	—	—	5	13	0.0035
15a	F	OH	F	H	2	5	0.261
15b	Br	OH	Br	H	4	3	0.015
15c	H	OH	H	H	8	12	12
15d	H	2-Morpholinoethoxy	OMe	H	9	8	0.163
15e	H	2-(Dimethylamino)ethoxy	H	H	3	22	0.466
15f	H	H	H	H	16	27	10
15g	H	2-Morpholinoethoxy	H	H	15	37	0.205
15h	H	2-(Diethylamino)ethoxy	OMe	H	24	26	—
15i	H	Acetamide	H	H	28	26	10
15j	H		OMe	H	24	26	—
15k	H	4-Methylpiperazin-1-yl	OMe	H	26	32	—
15l	H	4-Morpholino	OMe	H	33	22	—
15m	H	OMe	H	H	42	47	—
15n	H	2-(Dimethylamino)ethoxy	H	OMe	29	62	—
15o	H	3-(1H-tetrazol-5-yl)propoxy	H	H	38	85	—
15p	H	4-Methyl-1H-imidazol-1-yl	OMe	H	41	52	—
15q	H	Tosyl	OMe	H	48	50	—
15r	H	4-Methoxybenzoxonitrile	H	H	74	52	—
15s	H	Methyl 4-(methoxy)benzoate	H	H	85	89	—
15t	—	—	—	—	26	56	—

* Control.

Scheme 2. Synthesis of compounds **20a** and **20b**.

under basic conditions to obtain a number of structurally diverse compounds **9a–m** in good yields (see [Supporting information](#)).²⁰ Furthermore 4-fluoro-3-methoxybenzaldehyde **10** was connected to the corresponding cyclic amines **11a–c** and to its corresponding sulfonyl derivative **11d**. An aminoalkylation of 1*H*-indole-6-carbaldehyde **12** resulted in aldehyde **13**. The final condensation was carried out in a microwave reactor. The reaction of 5-chloroindolin-2-one **14** with the commercial and synthesized aldehydes yielded the indolinone derivatives **15a–t** in good yields up to 97% ([Table 2](#)).

The obtained indolinone derivatives **15a–t** were tested for their ability to inhibit LRRK2 kinase activity (assay conditions available in [Supporting data](#)).^{26,27} Indeed most of the synthesized indolinone derivatives **15a–t** exhibited good *in vitro* activity reducing LRRK2 activity below 50% at 10 μM ([Table 2](#)). Two exceptions are the derivatives **15r** and **15s**, which were unable to significantly reduce the *in vitro* LRRK2 activity (reduction to 74% and 85%, respectively). This may be caused by the length and the size of the second phenyl ring. On the contrary, indolinone derivatives which have no or a short substitution at the 4-hydroxyl of the phenol exhibited high potency against LRRK2 at a concentration of 10 μM . Three of them, the derivatives **15a–b** and **15d**, also reduced LRRK2 activity below 10% in the presence of 1 μM test compound. Additionally we determined the IC_{50} 's of selected indolinone derivatives ([Table 2](#)). Compound **15b** is highly potent against LRRK2 with an IC_{50} value of 15 nM. Interestingly, indolinone derivative **15b** is closely related to the known brain-penetrant, non-selective LRRK2 inhibitor GW5074 **1**, only the substitution to chlorine in the 5th position of the indol ring is different ([Fig. 1](#)). Remarkably this compound **15b** exhibited a 53-fold higher activity against LRRK2 than GW5074 **1** (IC_{50} of 880 nM).¹² Further impacts on the activity

of derivative **15b** have substitutions in the 3rd and 5th position of the phenol ring. Compounds **15c** and **15f**, which lack substitutions in this position, displayed a dramatic decrease in LRRK2 inhibitory activity ($\text{IC}_{50} = 12 \mu\text{M}$ and $\text{IC}_{50} = 10 \mu\text{M}$, respectively) in comparison to the compounds **15a–b** and **15d**.

The chlorine of lead compound **15b** was further substituted ([Scheme 2](#)). Two residues with different sizes were chosen to analyze the impact regarding LRRK2 activity on this position. Intermediate **17** was generated via Suzuki coupling between 5-bromoindolin-2-one **16** and benzeneboronic acid. Furthermore isatin **18** was reduced using hydrazine monohydrate to yield indolinone derivative **19**. The final compounds **20a** and **20b** were coupled via Knoevenagel condensation. The LRRK2 activities of compounds **20a** and **20b** are given in [Table 3](#). Derivative **20a**, carrying the phenyl residue, exhibited a 6-fold decrease in LRRK2 activity (0.204 μM) compared to its corresponding methoxy derivative **20b** with 0.031 μM LRRK2 inhibitory activity.

Next, docking studies were performed to analyze the potential binding mode of the most active LRRK2 inhibitor **15b**. Models of compound **15b** docked into the ATP-binding site of LRRK2 are shown in [Figures 3A](#) and [B](#). The indolinone core favorably interacts with the backbone of LRRK2. Especially glutamic acid 1948 is close to the N–H motif of the indole and forms a strong hydrogen bond, whereas the chlorine of the indolinone core binds towards the solvent exposed region of the ATP-binding site ([Fig. 3A](#) and [B](#)). More important are the interactions of the 3,5-dibromo-4-phenol moiety with the rear of the mostly hydrophobic binding pocket ([Fig. 3A](#) and [B](#)). Hydrophobic interactions were observed between the phenol ring and the gatekeeper residue M1947 in addition to several hydrophobic interactions with the 3,5-dibromo substitutions (e.g., L1924 and G1888). The 4-hydroxy group of the phenol turns

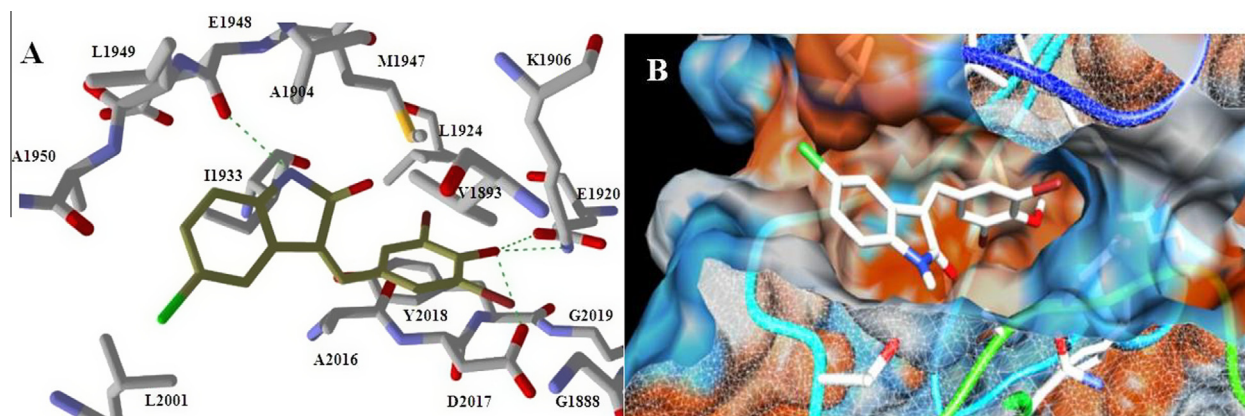
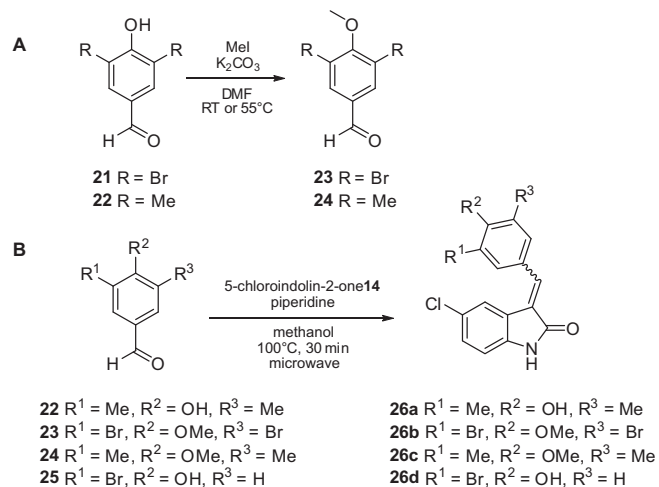


Figure 3. Suggested binding mode of compound **15b**. The homology model of LRRK2 was made using the Swiss Model server.^{24,25} The molecular docking was performed using the software Molegro Virtual Docker 6. (A) Compound **15b** (brown) docked in the ATP-binding site of LRRK2. Important interactions are shown as green dashed lines. (B) Surface illustration of the ATP-binding site of LRRK2 and the ligand **15b** (white).



Scheme 3. (A) Methylation of aldehydes **21** and **22** to its corresponding counterparts **23** and **24**. (B) Connecting the aldehydes with indolinone **14** via Knoevenagel condensation.

Table 3
Indolinone derivatives **20a** and **20b** and their in vitro LRRK2 inhibitory activity

Compound	R ¹	IC ₅₀ (μM)
20a	Ph	0.204
20b	OMe	0.031

Table 4
Synthesized indolinone derivatives and their in vitro LRRK2 inhibitory activity

Compound	R ¹	R ²	R ³	IC ₅₀ (wt LRRK2) (μM)	IC ₅₀ (LRRK2 G2019S)
15b	Br	OH	Br	0.015	0.010 μM
26a	Me	OH	Me	0.194	—
26b	Br	OMe	Br	>10	—
26c	Me	OMe	Me	1.5	—
26d	Br	OH	H	0.046	0.064 μM

out to be particularly important. As already speculated by Chen et al.,¹⁹ the 4-hydroxyl of the triazolopyridine **6** (Fig. 1) may act as a donor and as an acceptor, but this has not been proven. This interaction is also clearly represented in Figure 3A. On the one hand the 4-hydroxyl group of compound **15b** is donating two hydrogen bonds to the conserved residues E1920 and D2017, whereas it also acts as an acceptor by forming a strong H-bond with K1906.

To confirm the docking results and to confirm the importance of the hydroxyl group in the 4th position of the phenol ring a second

round of derivatization was performed. A replacement of the hydroxyl should result in loss of LRRK2 inhibitory activity. Therefore additional indolinone derivatives were synthesized (outlined in Scheme 3 and Table 4). The easiest way to establish the role of a hydroxyl in this position is replacement of the hydrogen atom by a methyl group. Therefore, in the presence of methyl iodide and potassium carbonate compound **21** was converted to its corresponding aldehyde **23**. Substitutions in the 3rd and 5th position of the phenol ring also influence LRRK2 inhibitory activity. The commercial 4-hydroxy-3,5-dimethylbenzaldehyde **22**, its corresponding methylated counterpart **24** and the commercial aldehyde **25** which carries only one bromine in the 3rd position were also coupled under the same Knoevenagel conditions with indolinone **14** in good yields between 77% and 89% (Scheme 3, Table 3).

The obtained indolinone derivatives **26a–d** were also tested for their ability to inhibit LRRK2 kinase activity in vitro (Table 4). As expected, the methylation of the phenol oxygen resulted in a dramatic loss of in vitro LRRK2 activity. The comparison of compounds **15b** and **26b** indicates a multiple drop of LRRK2 inhibitory activity from 0.015 μM to >10 μM. This was also confirmed by the indolinone derivatives **26a** and **26c**, respectively. The 3,5-dimethyl-4-hydroxy moiety of compound **26a** exhibited a reduced activity with an IC₅₀ of 0.194 μM relative to compound **15b** (IC₅₀ = 15 nM), but showed a 7 times higher activity concerning its corresponding methylated form **26c** with an IC₅₀ of 1.5 μM (Table 3). This confirms the importance of a hydroxyl in position R² (Table 1 and Table 3) for the inactivating activity of indolinone based compounds. Remarkably compound **26d**, which carries one bromine only, exhibited also high potency against LRRK2 with an IC₅₀ value of 0.046 μM.

G2019S, the most common disease-causing mutation in LRRK2 dramatically increased kinase activity. Additionally to the wild-type LRRK2 activity we determined the LRRK2 activity against the G2019S mutant for compounds **15b** and **26d** (Table 4). Both compounds inhibited the LRRK2 G2019S mutant in a similar manner as obtained for wild type LRRK2 with 0.010 μM for compound **15b** and 0.064 μM for compound **26d**, respectively.

The indolinone scaffold is well known of its activity in inhibiting several different classes of kinases. Therefore we next examined the kinase selectivity of lead compound **15b**. The kinase selectivity of compound **15b** was assessed against a panel (ExpresS Diversity kinase profile) of 46 human protein kinases (Fig. 4). At a concentration of 1 μM compound **15b** merely inhibited the serine/threonine kinases of HGK (MAPAK4) and Pimp2 with a residual activity below 30%. These results suggest that **15b** is a selective LRRK2 inhibitor, however further profiling against additional kinases are needed.

After the evaluation of the in vitro activity of this set of indolinone derivatives the most potent and promising compounds **15b** and **26d** were additionally tested for their in vivo activity on zebrafish embryos. The zebrafish (*Danio rerio*) has become a useful vertebrate model for assessing toxicological effects of chemicals and drugs and is standardized international.^{28,29} Rapid development of the embryos, their small size, high fecundity and the ease of husbandry are advantages of zebrafish for a pharmacological and toxicological research.^{28,30,31} Treatment of the zebrafish embryo with chemicals or drugs a phenotypic description of the zebrafish development provides data for compound permeability and safety.

The zebrafish embryos were collected and maintained in E3 medium at 28 °C. The indolinone derivatives **15b** and **26d** were added at 24 hpf (hours post fertilization) and the phenotypes were compared at 96 hpf (Fig. 5). At 20 μM compound **15b** caused a reduced growth compared to concentrations of 1, 5, 10 μM and the control (Fig. 5A–D and I). The zebrafish displayed stunted and crooked tails at a higher concentration of 30 μM. The lethality of the zebrafish was observed every 24 h up to 120 hpf. Above a

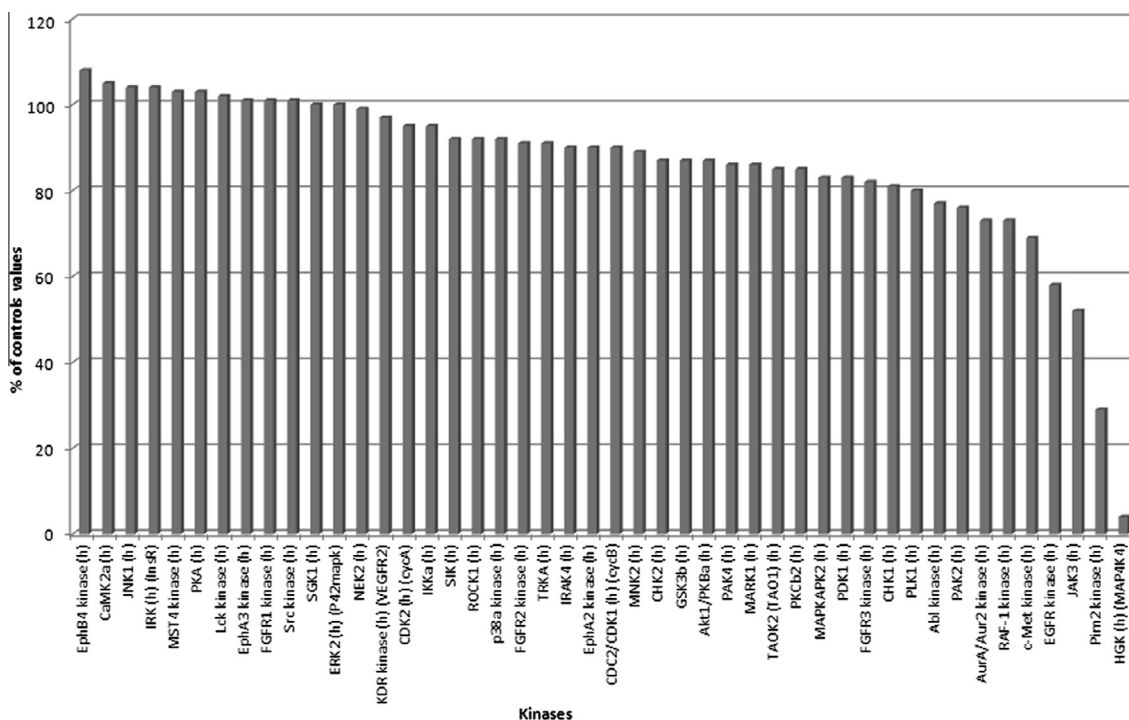


Figure 4. Screening of compound **15b** against 46 human protein kinases at 1 μM . Each bar represents the activity of one individual protein kinase (see [Supplementary data](#) for more details).



Figure 5. In vivo cytotoxicity with zebrafish embryos. The zebrafish embryos were collected and maintained in E3 medium at 28 °C. Compounds **15b** and **26d** were added 24 hpf (hours post fertilization) and the phenotypes were compared after 96 hpf. (A–E) Zebrafish embryos treated with compound **15b** in different concentrations of 1 μM (A), 5 μM (B), 10 μM (C), 20 μM (D) and 30 μM (E). (F–H) Exposure of the zebrafish embryos to 1 μM , 5 μM and 10 μM of **26d**. **26d** caused stunted and crooked tail at 5 μM , which is more pronounced at 10 μM . (I) Control embryo in 1% DMSO.

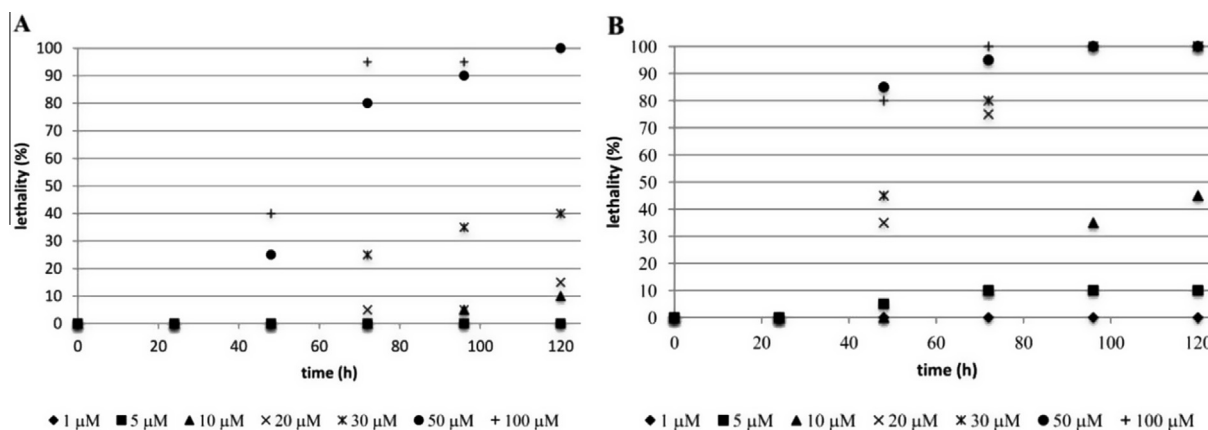


Figure 6. Lethality representation of the zebrafish embryos at different time points for indolinone derivative **15b** and **26d**. The observed data are expressed as averages of duplicates. (A) Lethality caused by compound **15b**. (B) Lethality caused by compound **26d**.

concentration of 30 μM **15b** we observed an increased lethality over time (Fig. 6A). After 120 hpf the lethality for concentrations of 50 μM and 100 μM of compound **15b** exhibited 100%, whereas at 30 μM 40% of the zebrafish embryos died. The zebrafish assay did not indicate any abnormalities and lethality at a concentration below 10 μM (Fig. 5A–D and 6). Related, but more distinct phenotypes were observed for compound **26d**. Reduced growth and stunted and crooked tails were already observed at a concentration of 5 μM , and this is more pronounced at 10 μM (Fig. 5G and H). Indolinone derivative **26d** also displayed a higher in vivo toxicity compared to **15b** (Fig. 6B). At a concentration above 10 μM the lethality increased dramatically over time. After 48 hpf the lethality of the zebrafish embryos increased over 80% for concentrations of 20 and 30 μM , respectively. Therefore, there is a window of safe treatment doses of these compounds situated below 5 μM and above 15 μM which may be used in evaluating neuroprotective effects.

The observed deformities of the zebrafish indicated evidences of exposure and cell penetration of the indolinone derivatives **15b** and **26d**. Nevertheless, it cannot be ruled out that the defects on the axis is an off-target effect via glycogen synthase kinase-3 (GSK-3) inhibition. It is known that Wnt signaling, and thus GSK-3 activity, plays a crucial role in the development of metazoan and was confirmed for known GSK-3 inhibitors, which interrupt zebrafish development.^{32–34} Interestingly, the eyeless phenotype caused by GSK-3 inhibitors,^{35,36} was not observed for both indolinone derivatives. Hence, we tested both compounds at 10 μM against GSK-3 α and GSK-3 β to find out whether they have the GSK-3 activity (assay information's are available in [Supplementary data](#)). Compound **15b** exhibited a moderate activity (GSK-3 α = 59%, GSK-3 β = 73%), whereas compound **26d** is inactive against both proteins (GSK-3 α = 30%, GSK-3 β = 19%). These results indicated that the observed phenotypes are not linked up with GSK-3 activity. Especially for compound **15b** the deformities of the phenotypes were observed at higher concentrations of 20 and 30 μM , respectively.

Therefore, the results of the zebrafish embryo phenotype assay indicate sufficient cell permeation of the compounds **15b** and **26d**.

In conclusion we have synthesized and evaluated a series of potent indolinones as LRRK2 inhibitors. Two of our most active and promising compounds **15b** and **26d** are characterized by an IC_{50} value of 15 and 46 nM against wild-type LRRK2 and 10 and 64 nM against the LRRK2 G2019S mutant, respectively. The combination of the docking studies and the LRRK2 in vitro results of **15b** illustrate the inhibitor-enzyme interaction with the ATP-binding pocket. We established that the hydrogen bond between the

4-hydroxy group of the phenol and the conserved residues E1920 and D2017 is essential for LRRK2 inhibition. During the development of drugs, safety is one of the most important factors. In our in vivo zebrafish embryo phenotype assay we have evaluated the toxicity of both compounds. We observed that indolinone derivative **15b** displayed no significant toxicity below 10 μM , whereas compound **26d** displayed an increased toxicity over time.

Further improvements are required to pursue with more detail phenotypic testing of analogues compounds in vivo and enable development in preclinical models.

Acknowledgment

The authors thank the Hans und Ilse Breuer Stiftung for financial support.

Supplementary data

Supplementary data associated with this article can be found, in the online version, at <http://dx.doi.org/10.1016/j.bmcl.2014.08.049>.

References and notes

- Lee, B. D.; Dawson, V. L.; Dawson, T. M. *Trends Pharmacol. Sci.* **2012**, *33*, 365.
- Tong, Y.; Shen, J. *Neuron* **2009**, *64*, 771.
- Kramer, T.; Lo Monte, F.; Göring, S.; Okala Amombo, G. M.; Schmidt, B. *ACS Chem. Neurosci.* **2012**, *3*, 151.
- Taymans, J. M.; Cookson, M. R. *BioEssays: News Rev. Mol., Cell. Dev. Biol.* **2010**, *32*, 227.
- Cookson, M. R. *Nat. Rev. Neurosci.* **2010**, *11*, 791.
- Seol, W. *BMB Rep.* **2010**, *43*, 233.
- Greggio, E.; Jain, S.; Kingsbury, A.; Bandopadhyay, R.; Lewis, P.; Kaganovich, A.; van der Brug, M. P.; Beilina, A.; Blackinton, J.; Thomas, K. J.; Ahmad, R.; Miller, D. W.; Kesavapany, S.; Singleton, A.; Lees, A.; Harvey, R. J.; Harvey, K.; Cookson, M. R. *Neurobiol. Dis.* **2006**, *23*, 329.
- Nichols, R. J.; Dzakmo, N.; Morrice, N. A.; Campbell, D. G.; Deak, M.; Ordureau, A.; Macartney, T.; Tong, Y.; Shen, J.; Prescott, A. R.; Alessi, D. R. *Biochem. J.* **2010**, *430*, 393.
- West, A. B.; Moore, D. J.; Biskup, S.; Bugayenko, A.; Smith, W. W.; Ross, C. A.; Dawson, V. L.; Dawson, T. M. *Proc. Natl. Acad. Sci. U.S.A.* **2005**, *102*, 16842.
- Daniels, V.; Baekelandt, V.; Taymans, J. M. *Neuro-Signals* **2011**, *19*, 1.
- Dusonchet, J.; Kochubey, O.; Stafa, K.; Young, S. M., Jr.; Zufferey, R.; Moore, D. J.; Schneider, B. L.; Aebischer, P. *J. Neurosci.* **2011**, *31*, 907.
- Lee, B. D.; Shin, J. H.; VanKampen, J.; Petrucelli, L.; West, A. B.; Ko, H. S.; Lee, Y. I.; Maguire-Zeiss, K. A.; Bowers, W. J.; Federoff, H. J.; Dawson, V. L.; Dawson, T. M. *Nat. Med.* **2010**, *16*, 998.
- Taymans, J. M. *Expert Opin. Ther. Pat.* **2014**, *24*, 727.
- Vancraenenbroeck, R.; Lobbstaal, E.; Maeyer, M. D.; Baekelandt, V.; Taymans, J. M. *CNS Neurol. Disord.: Drug Targets* **2011**, *10*, 724.
- Deng, X.; Dzakmo, N.; Prescott, A.; Davies, P.; Liu, Q.; Yang, Q.; Lee, J. D.; Patricelli, M. P.; Nomanbhoy, T. K.; Alessi, D. R.; Gray, N. S. *Nat. Chem. Biol.* **2011**, *7*, 203.

16. Zhang, J.; Deng, X.; Choi, H. G.; Alessi, D. R.; Gray, N. S. *Bioorg. Med. Chem. Lett.* **2012**, *22*, 1864.
17. Choi, H. G.; Zhang, J.; Deng, X.; Hatcher, J. M.; Patricelli, M. P.; Zhao, Z.; Alessi, D. R.; Gray, N. S. *ACS Med. Chem. Lett.* **2012**, *3*, 658.
18. Garofalo, A. W.; Adler, M.; Aubele, D. L.; Bowers, S.; Franzini, M.; Goldbach, E.; Lorentzen, C.; Neitz, R. J.; Probst, G. D.; Quinn, K. P.; Santiago, P.; Sham, H. L.; Tam, D.; Truong, A. P.; Ye, X. M.; Ren, Z. *Bioorg. Med. Chem. Lett.* **2013**, *23*, 71.
19. Chen, H.; Chan, B. K.; Drummond, J.; Estrada, A. A.; Gunzner-Toste, J.; Liu, X.; Liu, Y.; Moffat, J.; Shore, D.; Sweeney, Z. K.; Tran, T.; Wang, S.; Zhao, G.; Zhu, H.; Burdick, D. J. *J. Med. Chem.* **2012**, *55*, 5536.
20. Amombo, G. M.; Kramer, T.; Lo Monte, F.; Göring, S.; Fach, M.; Smith, S.; Kolb, S.; Schubengel, R.; Baumann, K.; Schmidt, B. *Bioorg. Med. Chem. Lett.* **2012**, *22*, 7634.
21. Mahboobi, S.; Uecker, A.; Sellmer, A.; Cenac, C.; Hocher, H.; Pongratz, H.; Eichhorn, E.; Hufsky, H.; Trumpler, A.; Sicker, M.; Heidel, F.; Fischer, T.; Stocking, C.; Elz, S.; Bohmer, F. D.; Dove, S. *J. Med. Chem.* **2006**, *49*, 3101.
22. Schmidt-Arras, D.; Schwable, J.; Bohmer, F. D.; Serve, H. *Curr. Pharm. Des.* **2004**, *10*, 1867.
23. Troxler, T.; Greenidge, P.; Zimmermann, K.; Desrayaud, S.; Druckes, P.; Schweizer, T.; Stauffer, D.; Rovelli, G.; Shimshek, D. R. *Bioorg. Med. Chem. Lett.* **2013**, *23*, 4085.
24. Arnold, K.; Bordoli, L.; Kopp, J.; Schwede, T. *Bioinformatics* **2006**, *22*, 195.
25. Kiefer, F.; Arnold, K.; Kunzli, M.; Bordoli, L.; Schwede, T. *Nucleic Acids Res.* **2009**, *37*, D387.
26. Vancraenenbroeck, R.; De Raeymaecker, J.; Lobbstaël, E.; Gao, F.; De Maeyer, M.; Voet, A.; Baekelandt, V.; Taymans, J. M. *Front. Mol. Neurosci.* **2014**, *7*, 51.
27. Taymans, J. M.; Vancraenenbroeck, R.; Ollikainen, P.; Beilina, A.; Lobbstaël, E.; De Maeyer, M.; Baekelandt, V.; Cookson, M. R. *PLoS ONE* **2011**, *6*, e23207.
28. Giannaccini, G.; Cuschieri, A.; Dente, L.; Raffa, V. *Nanomed: Nanotechnol., Biol., Med.* **2014**, *10*, 703–719.
29. Lammer, E.; Carr, G. J.; Wendler, K.; Rawlings, J. M.; Belanger, S. E.; Braunbeck, T. *Comp. Biochem. Physiol. C* **2009**, *149*, 196.
30. Deeti, S.; O'Farrell, S.; Kennedy, B. N. *J. Pharmacol. Toxicol. Methods* **2014**, *69*, 1.
31. Taylor, K. L.; Grant, N. J.; Temperley, N. D.; Patton, E. E. *Cell Commun. Signal* **2010**, *8*, 11.
32. Atilla-Gokcumen, G. E.; Williams, D. S.; Bregman, H.; Pagano, N.; Meggers, E. *Chembiochem: Eur J. Chem. Biol.* **2006**, *7*, 1443.
33. Lo Monte, F.; Kramer, T.; Gu, J.; Anumala, U. R.; Marinelli, L.; La Pietra, V.; Novellino, E.; Franco, B.; Demedts, D.; Van Leuven, F.; Fuertes, A.; Dominguez, J. M.; Plotkin, B.; Eldar-Finkelman, H.; Schmidt, B. *J. Med. Chem.* **2012**, *55*, 4407.
34. Paquet, D.; Bhat, R.; Sydow, A.; Mandelkow, E. M.; Berg, S.; Hellberg, S.; Falting, J.; Distel, M.; Koster, R. W.; Schmid, B.; Haass, C. *J. Clin. Invest.* **2009**, *119*, 1382.
35. Finkelsztein, A.; Kelly, G. M. *Biol. Cell* **2009**, *101*, 661–664 p following 678.
36. Zhong, H.; Zou, H.; Semenov, M. V.; Moshinsky, D.; He, X.; Huang, H.; Li, S.; Quan, J.; Yang, Z.; Lin, S. *Mol. Biosyst.* **2009**, *5*, 1356.